Heat Mass Transfer (2006) 43: 7–15
DOI 10.1007/s00231-005-0080-8

ORIGINAL

H. Umur · A. A. Ozalp

Fluid flow and heat transfer in transitional boundary layers: effects of surface curvature and free stream velocity

Received: 16 September 2004 / Accepted: 8 December 2005 / Published online: 1 February 2006

Abstract Velocity and wall temperature measurements, over flat plate, concave and convex walls, were experimentally investigated in a low-speed wind tunnel with inlet velocities of 4 and 12 m/s encompassing the transitional region with streamwise distance Reynolds numbers from 3.15×10^5 to 1.04×10^6. As the velocity profiles, recorded by a semi-circular pitot tube and a digital constant-temperature hot-wire anemometer, were compared to exact Blasius profile and (1/7)th power law, experimental local Stanton numbers to analytical flat plate solution and turbulent correlation formula. Intermittency factors, derived from velocities and local Stanton numbers, were presented both in streamwise and pitchwise directions. It was found that the convex curvature delayed transition up to $Re_x = 1.04\times10^6$, with a mean intermittency value of 0.61 and a shape factor of 1.81, where the similar intermittency and shape factors were determined at Re_x of 8.33×10^5 and 4.25×10^5 for the flat plate and concave wall, indicating the enhancing role of concave curvature on the transition mechanism. The thinner boundary layers of the concave surface resulted in higher intermittency values, corresponding to higher skin friction and Stanton numbers; moreover the lowest gap between the measured and derived Stanton numbers were also obtained over the concave surface. Destabilising role of the concave wall caused Stanton numbers to increase up to 22%, whereas the convex wall, due to its stabilising character, produced lower Stanton numbers by 12% with respect to those of the flat plate.

H. Umur (✉) · A. A. Ozalp
Department of Mechanical Engineering, University of Uludag,
16059 Gorukle, Bursa, Turkey
E-mail: umur@uludag.edu.tr
Tel.: +90-224-4428877
Fax: +90-224-4428877

List of symbols

A, a, b, c	correlation constants (dimensionless)
C_f	skin friction (dimensionless)
C_p	constant pressure specific heat (J/kg K)
h	heat transfer coefficient (W/m^2 K)
H	shape factor (dimensionless)
q	heat flux (W/m^2)
Pr	Prandtl number (dimensionless)
R	radius of curvature (cm)
Re_x	streamwise distance Reynolds number (dimensionless)
Re_θ	momentum thickness Reynolds number (dimensionless)
St	Stanton number (dimensionless)
T_w	wall temperature (°C)
T_o	free stream temperature (°C)
Tu	turbulence level (%)
u	streamwise velocity (m/s)
U	mean free stream velocity (m/s)
x, y, z	streamwise, pitchwise and spanwise directions (mm)
x_l	unheated starting length (mm)

Greek

δ	boundary layer thickness (mm)
φ	transition parameter (dimensionless)
γ	local intermittency factor (dimensionless)
$\bar{\gamma}$	mean intermittency factor (dimensionless)
θ	momentum thickness (mm)
ν	kinematic viscosity (m^2/s)
ρ	density (kg/m^3)
τ_w	wall shear stress (Pa)

Subscripts

o	flow-off
f	flow-on
L	laminar

T turbulent
te transition end
ts transition onset

1 Introduction

Flow and heat transfer characteristics with transitional flows are of great importance for the design process of a wide range of practical applications, including compressor and turbine blades, cooling vanes and heat exchangers, since the transition plays a significant role on the enhancement of the local wall shear stress and convective heat transfer rates. Straight and curved surfaces are of great importance because they provide environments to investigate an assortment of transitional phenomena and they are highly influential on the start and end of transition process; in terms of velocity and heat transfer parameters.

Flat wall is the most common flow surface and the regarding transitional flow characteristics have been extensively investigated. Narasimha [1] derived an analytical solution for the intermittency distribution by assuming that all the turbulent spots originate from one streamwise position in the laminar boundary layer. The natural transition of flat plate boundary layers were investigated by Abu-Ghannam and Shaw [2] and they proposed empirical correlations for the prediction of start and end of transition region. Cheng et al. [3] experimented the convective heat transfer in transitional flow and their Stanton numbers deviated from the turbulent correlation by 19–59%. Intermittency effects on convective heat transfer were experimentally investigated by Zumbrunnen and Aziz [4], who reported that intermittent flows yielded enhancements in convective heat transfer rates by a factor of 2. Ciofalo et al. [5] studied flow and heat transfer characteristics of plate heat exchangers under transitional and weakly turbulent flows and determined the Nusselt number to correlate positively with Reynolds number and the friction factor to be less influenced by Reynolds number towards downstream. Earlier transition and reduced transition length due to high free stream turbulence were indicated by Zhou and Wang [6]. Hydrodynamic and thermal development of transitional boundary layers were investigated by Wang et al. [7], where the transitional momentum thickness-based Reynolds number (Re_θ) was in the range of 490–1,300 and the shape factor (H) was 1.4 at the end of transition. Johnson and Ercan [8] investigated the transitional flow and evaluated the shape factor data for the intermittency rates (γ) of 0.50, 0.75 and 0.99 as 1.9–2.0, 1.65–1.75 and 1.4–1.45, respectively. Fluid mechanics measurements of Vasudevan and Dey [9] pointed out thicker boundary layers, due to the decrease of spanwise measure of the test section in the flow direction, where their turbulent H was around 1.5 for $\gamma = 0.97$. Schook et al. [10] reported that for the flow cases with high intermittency values, the end of transition can be located at a relatively low Reynolds number of $\mathrm{Re}_x < 2.0\times10^5$, however, at the end of transition their heat transfer data coincided with the turbulent correlation regardless of the intermittency level.

Due to the destablising character and being the pressure side of the turbine blades concave surface boundary layers have been under consideration particularly from the point of instabilities, which occur especially during transition from laminar to turbulent flow. Zhang et al. [11] experimented a 2 m curvature for laminar and transitional flows and reported intermittency to grow rapidly in the early stages of transition and to decrease in the pitchwise direction sharply for $y > 0.4\delta$. However, the flat plate records of Zhang et al. [12] pointed out the location of maximum intermittency at $y/\delta \approx 0.55$ and the intermittency values could only attain the minimum zero outside the boundary layer at $y/\delta \approx 1.25$. Volino and Simon [13] carried out fluid mechanics measurements over a 97 cm curvature and determined that intermittency exhibited peaks near the locations of the minima in the velocity profiles. The pitchwise intermittency reports of Kestoras and Simon [14] indicated a nearly constant value of 1 up to $y/\delta \approx 0.65$ and vanishing towards 0 around $y/\delta \approx 1.50$. Toe et al. [15] experimented the transitional region with free stream velocities of 2–9 m/s, and determined that the onset of transition shifts downstream with lower velocities. Conditional data sampling of Volino et al. [16] put forward the dissimilarity of the turbulent and non-turbulent zone velocity profiles, moreover, skin friction coefficients were 70% higher in the turbulent zone.

Suction side of the turbine blades and inner surface of heat exchanger channels are of convex curvature type and devoted to its stabilizing character as much as 50–80% of the surface can be covered with flow undergoing transition. Turbulent flow over a 2,410 mm radius was experimentally investigated by Muck et al. [17], who determined that at $y/\delta = 0.6$ the intermittency factor was around 0.9 which was followed by a sudden drop for $y/\delta > 0.6$. Wang and Simon [18] worked on two distinct convex curvatures and determined that the transitional heat transfer rates of the convex surfaces were lower than the flat wall measurements by around 60 and 40% for the curvatures of 180 and 90 cm, respectively. Abu-Qudais et al. [19] reported, for the convex section of a parabolic cylinder, augmented skin friction distributions with higher Reynolds number and monotonic decrease of heat transfer rates in streamwise direction. Turbulent flow characteristics over the convex side ($R = 492$ mm) of a swept bump were experimentally considered by Webster et al. [20], who reported Re_θ and H to increase in the flow direction with ranges of 3,100–6,100 and 1.21–1.62, respectively. Ligrani and Hedlund [21] performed flat and convex surface experiments, where the flat plate heat transfer values were above those of the convex wall by 25%. Unsteadiness effects on convex and

concave surface flows were handled by Wright and Schobeiri [22]; who determined the concave wall to be more influenced than the convex wall, with higher heat transfer rates and earlier transition. Turner et al. [23] experimented the 1,200 mm curvature with two inlet velocities and recorded 45% augmented heat transfer rates for the higher inlet velocity case.

The above-defined past research has contributed much to the understanding of transitional flows, however, issues requiring further study include the combined handling of flat and curved surfaces in transitional flows, with more than one inlet velocity to provide a deeper understanding on the mechanisms of transition from laminar to turbulent flow. Ozalp and Umur [24] experimentally investigated the flat, concave and convex wall boundary layers both in laminar and turbulent flows and experimented boundary layer development in conjunction with surface heat transfer rates. The current work has been carried out over the identical surfaces of the former study of the authors, to bridge the gap between laminar and turbulent flows by considering both the flow and heat transfer characteristics of the transition mechanism.

2 Experimental details

The general arrangement of the low-speed wind tunnel used for the present experimental program is in Fig. 1. Air was drawn by an axial blower through a filter, a honey comb, a screen pack, a nozzle and a straight section, where the maximum air velocity at the inlet of the rectangular test section was 30 m/s with a turbulent intensity of less than 1%. The nozzle has a 3:1 contraction ratio providing a 300×200 mm exit area identical to the inlet of the test section. Honeycomb and screen packs in the upstream of the contraction ensured parallel streamlines with absence of swirl. Velocity measurements in the working section were made using a standard semi-circular pitot probe in conjunction with static pressure tappings on the flow wall, static pressures were recorded by a micro-manometer, where the overall estimated uncertainty of velocity measurements were less than $\pm 3\%$. While the turbulence level of around 1% at the inlet of the test section remained almost constant in the downstream direction for the flat plate case, that increased up to 1.2% for the concave and decreased to 0.8% for the convex curvatures at the end of the test section.

The rectangular test section of flat plate, concave and convex walls were manufactured at Uludag University, where the streamwise distance of the flat plate and curved walls were 750 and 1,000 mm, respectively. The radius of both curvatures was 1,500 mm providing a sufficiently high δ/R ratio to impose the influences of concave and convex cases on boundary layer development. As velocity profiles were attained at six different streamwise x-locations of 60, 180, 300, 420, 540 and 660 mm, surface temperature measurements were performed both at these profile stations and additionally at the midways, resulting in a total of 11 points to provide detailed and sufficient knowledge on the heat transfer mechanism. The copper plate, mounted on the bottom side of the test wall (Fig. 1) had a spanwise width of 240 mm and was heated by an electrical resistance (a high-current, low-voltage transformer) to obtain constant heat flux condition throughout the measurements. The wall and free stream temperatures were recorded by copper–constantan thermocouples and the heat loss through the backside of walls was minimised by fibreglass insulation. Heat transfer coefficient was defined as $h = q/(T_w - T_o)$ and the corresponding experimental

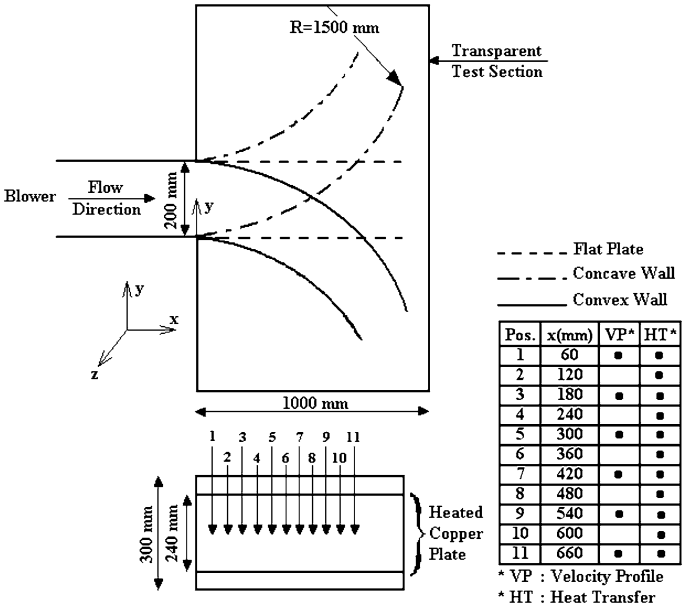

Fig. 1 Experimental setup

Stanton number by $St = h/(\rho\ U\ C_p)$ where $q = q_F - q_o$, q_F and q_o refer to flow-on and flow-off powers, ρ and C_p are the density and specific heat of fluid. In this particular case, the cumulative uncertainty of the experimental Stanton number is directly estimated by the equation of

$$\frac{\partial St}{St} = \left[\left(\frac{\partial U}{U}\right)^2 + \left(\frac{\partial q}{q}\right)^2 + \left(\frac{\partial T}{T}\right)^2 + \left(\frac{\partial \rho}{\rho}\right)^2 + \left(\frac{\partial C_p}{C_p}\right)^2\right]^{\frac{1}{2}}$$

and hence the maximum uncertainty in heat transfer measurements is found to be $\pm 4\%$.

3 Results and discussion

Velocity and wall temperature measurements were carried out over flat plate, concave and convex walls at constant heat flux condition with core flow velocities of 4 and 12 m/s corresponding to the complete transitional region. Velocity measurements were presented in non-dimensional form of u/U, compared to exact Blasius profile for laminar and to Prandtl approximation of (1/7)th power law for turbulent flow. Moreover $H\ (=\delta^*/\theta)$, where δ^* and θ refer to displacement and momentum thickness values respectively, γ and $\bar{\gamma}$ are also plotted with respect to y/δ and φ, where δ is experimentally determined at each profile location. Temperature measurements were presented as Stanton numbers derived from both C_f and measured wall and free stream temperatures together with flat-plate laminar analytical solution and turbulent correlation. Lastly $Re_\theta (= U\theta/\nu)$ and $Re_x\ (= Ux/\nu)$ were given in tabulated form, where the unheated starting length (x_l) was also taken into consideration in Reynolds number calculations by applying the Blasius profile of Eq. (1) to the initial measurement station with the boundary layer thickness value of $\delta_{x=60\ mm}$.

3.1 Velocity measurements

Dimensionless velocity profiles are recorded at streamwise distance of 60, 180, 300, 420, 540 and 660 mm of concave, flat and convex surfaces and presented in Fig. 2 at three stations of 60, 420 and 660 mm. While velocity profiles at 4 m/s remained close to Blasius profile where H ranged from 1.8 to 2.7, those of 12 m/s approached (1/7)th turbulent approximation with H values of 1.3–2.07. Where dimensionless Blasius profile is defined as

$$\eta = y\sqrt{\frac{U}{\nu x}} \quad \text{and} \quad \frac{\delta}{x} = \frac{5}{Re_x^{0.5}} \tag{1}$$

and Prandtl (1/7)th power law approximation by

$$\frac{u}{U} = \left(\frac{y}{\delta}\right)^{1/7} \quad \text{and} \quad \frac{\delta}{x} = \frac{0.37}{Re_x^{0.2}}. \tag{2}$$

As the flat plate velocity profiles are similar to those of Cheng et al. [3] and Vasudevan and Dey [9], Wright and Schobeiri's [22] concave surface measurements are in harmony with the current reports. The deviation of convex velocity profiles from the Blasius profile particularly $y/\delta > 0.8$ showed that surface curvature is of importance for the boundary layer development even at the first measuring station of 60 mm which gave rise to higher H values of around 2.7 than those of the concave and flat surfaces. The convex curvature effect became more pronounced at the lower velocity of 4 m/s than the higher one of 12 m/s.

In the downstream direction, the measured velocities approached (1/7)th power law, particularly on concave wall where H reduced to 1.8 and 1.3 in the flows with inlet velocities of 4 and 12 m/s, respectively. However, even at the last measuring station the H value of the convex wall was around 1.81, having a considerable distance from the turbulent flat plate value of 1.3,

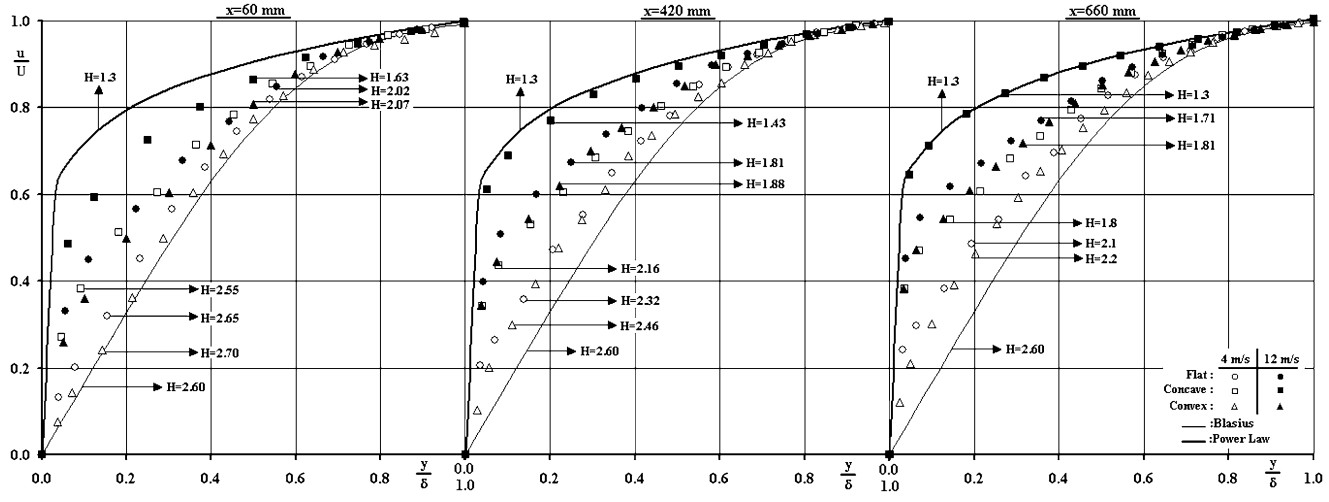

Fig. 2 Dimensionless velocity profiles

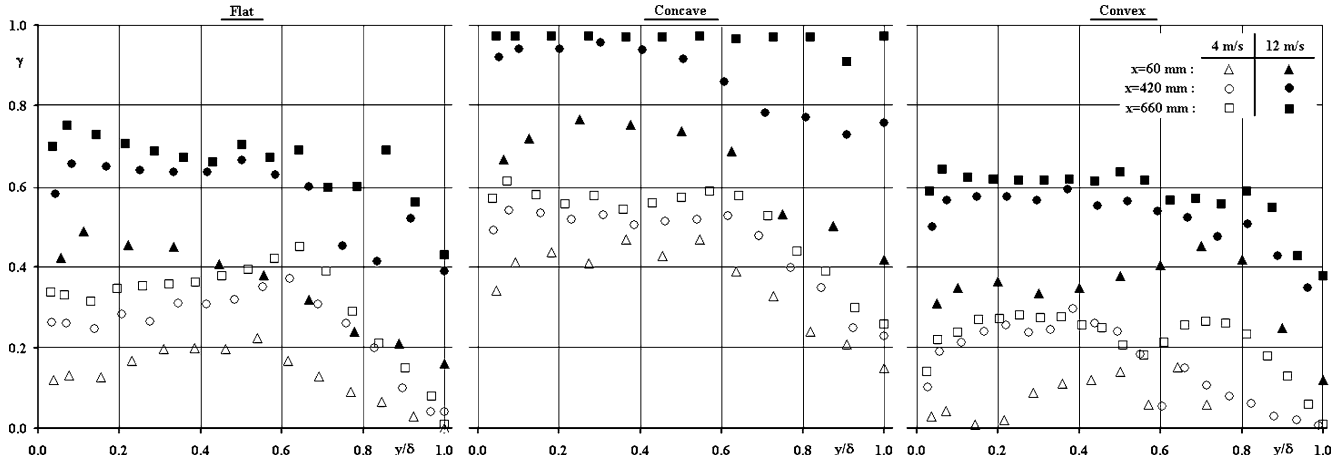

Fig. 3 Pitchwise variation of local intermittency factors

moreover, the downstream convex velocity profile for the 12 m/s case is significantly different from the turbulent records of Webster et al. [20] verifying the transitional character of the present measurements. These results were strongly supported by the intermittency profiles (γ) as plotted in Fig. 3. For instance, the intermittency profiles remained below 0.25 and 0.65 for the convex wall, 0.45–0.75 for flat plate and reached higher values of 0.65–0.97 for concave wall at 4 and 12 m/s, respectively. Muck et al.'s [17] turbulent intermittency measurements over a convex surface showed nearly a constant value of $\gamma = 1$ for $y \leq 0.4\delta$ and $\gamma = 0$ could only be reached outside the boundary layer at $y \approx 1.2\delta$. The current reports of lower intermittency data for the convex wall is an evidence of the transitional character and transition delaying role, where similar findings were also reported by Wang and Simon [18] by considering two distinct convex curvatures. The intermittency factor characterizes the transition region and is described by

$$\gamma = \frac{u - u_B}{u_T - u_B} \tag{3}$$

where $\gamma = 0$ refers to laminar flow, $\gamma = 1$ to turbulent flow, u is the local velocity, u_B and u_T present Blasius and turbulent velocities. The lower γ values coincide with higher H values for each case and the lower concave and larger convex wall values of H (the opposite is true for γ) than those of flat plate became more apparent towards the downstream so that H decreased up to 2.2–1.8 for the convex and to 1.8–1.3 for the concave surfaces at the last measuring station, for 4 and 12 m/s, respectively. As given in Fig. 3, the variation of intermittency with y/δ illustrates that γ started to rise from 0.2 and 0.4 and reached the highest values of 0.65 and 0.97 around $y/\delta = 0.65$ for the concave surface for 4 and 12 m/s, respectively. Similar to these findings, Zhang et al. [12] reported a maximum intermittency of 0.75 at $y/\delta \approx 0.55$, moreover, Kestoras and Simon [14] and Volino and Simon [13] determined a sharp decrease in intermittency for $y/\delta \geq 0.60$ and $y/\delta \geq 0.50$, respectively. The present measurements and the information from the literature show parallelism and can be attributed to the fact that the most effective turbulent activity occurs after midway across the boundary layer at $0.55 \leq y/\delta \leq 0.65$ and the concave wall intermittency profiles are fuller than flat plate and convex surface, as expected.

As can be seen from Tables 1 and 2, mean intermittency factors for all cases, calculated as

$$\bar{\gamma} = \frac{1}{\delta}\int_0^{\delta} \gamma \, dy \tag{4}$$

and increased with decreasing shape factor in the downstream direction together with increasing Re_θ at both case. The higher the H the lower the $\bar{\gamma}$, and H

Table 1 Boundary layer parameters at profile locations for $U = 4$ m/s

	Flat surface				Concave wall				Convex wall			
x (mm)	$\bar{\gamma}$	H	Re_θ	$Re_x(\times 10^5)$	$\bar{\gamma}$	H	Re_θ	$Re_x(\times 10^5)$	$\bar{\gamma}$	H	Re_θ	$Re_x(\times 10^5)$
60	0.14	2.65	280	3.75	0.37	2.55	230	3.15	0.06	2.7	360	4.40
180	0.19	2.59	310	4.05	0.40	2.43	260	3.46	0.08	2.63	390	4.71
300	0.23	2.45	350	4.36	0.45	2.3	295	3.76	0.11	2.55	430	5.01
420	0.26	2.32	390	4.67	0.46	2.16	330	4.07	0.16	2.46	480	5.32
540	0.29	2.2	430	4.97	0.47	2.01	370	4.38	0.18	2.33	530	5.63
660	0.32	2.1	480	5.28	0.52	1.8	420	4.68	0.22	2.2	590	5.93

Table 2 Boundary layer parameters at profile locations for $U = 12$ m/s

	Flat surface				Concave wall				Convex wall			
x (mm)	$\bar{\gamma}$	H	Re_θ	$Re_x(\times 10^5)$	$\bar{\gamma}$	H	Re_θ	$Re_x(\times 10^5)$	$\bar{\gamma}$	H	Re_θ	$Re_x(\times 10^5)$
60	0.36	2.02	720	5.20	0.65	1.63	672	4.25	0.35	2.07	750	6.74
180	0.45	1.91	792	5.98	0.79	1.56	699	5.17	0.44	1.95	834	7.48
300	0.52	1.84	882	6.77	0.81	1.49	726	6.09	0.49	1.9	948	8.24
420	0.58	1.81	990	7.55	0.88	1.43	756	7.01	0.51	1.88	1080	8.96
540	0.59	1.76	1086	8.33	0.92	1.38	792	7.92	0.57	1.82	1218	9.68
660	0.66	1.71	1200	9.10	0.97	1.3	840	8.84	0.61	1.81	1350	10.40

exceeded the laminar flat plate value of 2.6 on convex ($\bar{\gamma} = 0.06$, $H = 2.7$ and $Re_\theta = 360$) and H reached the turbulent value of 1.3 on concave wall ($\bar{\gamma} = 0.97$ and $Re_\theta = 840$), respectively. The convex curvature, where thicker boundary layers, corresponding to higher H, Re_θ and lower $\bar{\gamma}$, showed that convex surface itself retarded transition, while concave surface which led to fuller velocity profiles, smaller H and bigger $\bar{\gamma}$ values enhanced it, similar to those of Abu-Ghannam and Shaw [2]. The Re_θ range of 280–1,200 for the flat plate is in harmony with the findings of Wang et al. [7], pointing 492–1,302, however, above the upper limit ($(Re_\theta)_{te} = 900$) of Johnson and Ercan [8]. Table 2 indicates that even Re_x reached a value of 9.1×10^5 at the downstream section of the flat plate with the inlet velocity of 12 m/s, $\bar{\gamma}$ and H, values of 0.66 and 1.71 keep the flow still in the transition region. Wang et al. [7] determined the end of transition with H of 1.4 at $Re_x = 11.2\times10^5$ and Schook et al. [10] at $Re_x = 6\times10^5$ which are also above the critical Re_x of 5×10^5. Volino and Simon [13] indicated the end of transition with $Re_\theta = 500$ for the concave surface with $R = 97$ cm, on the other hand, the current corresponding data for $R = 150$ cm curvature is $Re_\theta = 840$ and put forth the influence of concave curvature on the transition mechanism from the point of boundary layer development. The H range of the convex wall is given as 2.7–1.81 (Tables 1, 2) and is above the turbulent establishments of Webster et al. [20] with 1.21–1.62, clarifying both the transitional character of the flow and stabilising role of the convex surface. Tables 1 and 2, moreover, demonstrates that the upstream $\bar{\gamma}$ and Re_θ values of the 12 m/s case are higher than those of the 4 m/s flow, which indicates that high inlet velocities enhance transition on both straight and curved surfaces and these findings are also in harmony with Toe et al.'s [15] reports for the concave wall.

The favourable effect of concave curvature on transition can also be seen in Fig. 4, where the mean $\bar{\gamma}$ values of 0.40 ($\varphi = 0.4$) and of 0.97 (($\varphi = 0.90$) occurred in concave wall much higher than those of convex wall and flat plate. The dimensionless parameter of φ is calculated as

$$\varphi = \frac{x - x_{ts}}{x_{te} - x_{ts}}, \tag{5}$$

where x_{ts} and x_{te} refer to start and end of transition, which indicate the streamwise locations with the intermittency values of $\bar{\gamma} = 0.00$ and 0.99, respectively, similar to the application of Gostelaw et al. [25]. In the convex and flat surface cases, where transition end locations ($\bar{\gamma} = 0.99$) were not reached experimentally, the x_{te} values are evaluated by extrapolating the available streamwise $\bar{\gamma}$ data, which was also applied by Gostelow et al. [25]. The distribution of the flat plate $\bar{\gamma}$ values show similarity with the reports of Schook et al. [10] and the $\bar{\gamma}$ values remained between the analytical solutions of Abu-Ghannam and Shaw [2], Schubauer and Klebanoff [26] and Narasimha [1]. The best fit led to the expression of

$$\bar{\gamma} = 1 - \exp(-4\varphi^2), \tag{6}$$

which can be used for the definition of $\bar{\gamma}$ as a function of transition parameter φ, with an error of less than $\pm 2\%$.

3.2 Heat transfer measurements

Temperature measurements at constant heat flux condition were taken at 11 locations in the downstream direction from 60 to 660 mm, while velocity measurements were obtained at six stations. Temperature measurements have been presented in Stanton number form, as seen in Figs. 5 and 6 and the experimental Stanton numbers were compared to St derived from skin friction

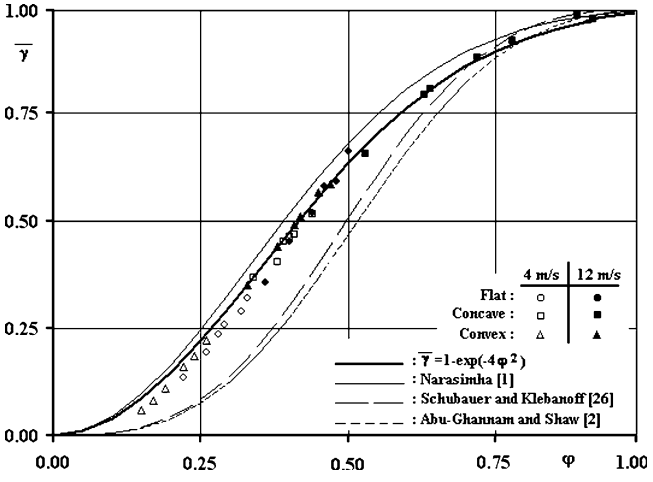

Fig. 4 Variation of mean intermittency factors with transition parameter

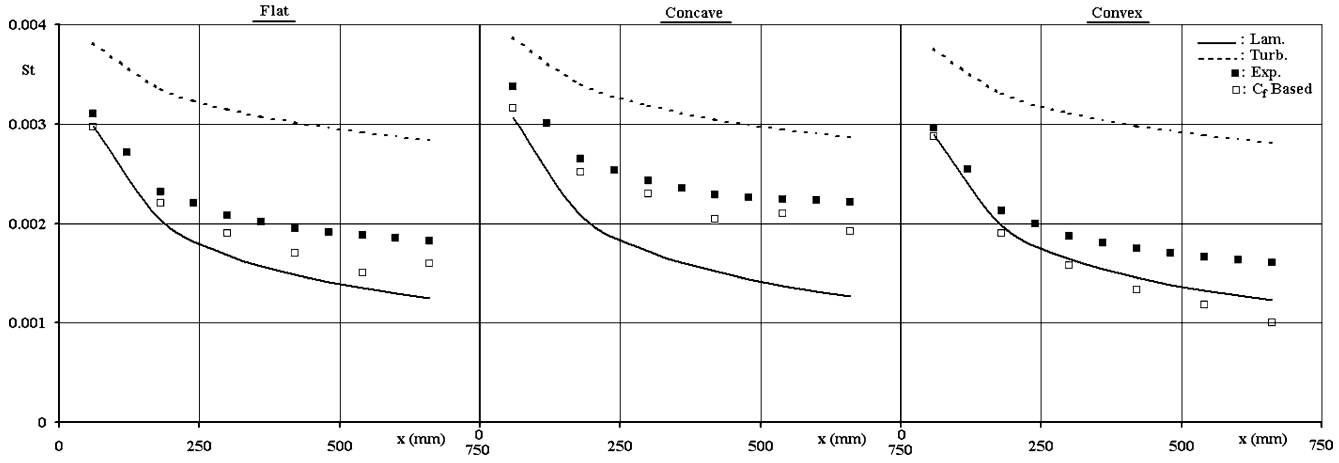

Fig. 5 Streamwise variation of Stanton numbers for $U = 4$ m/s

($C_f/2$), and to laminar analytical solution and turbulent correlation formula. Skin friction C_f is derived from velocity profiles as $C_f = \tau_w/0.5\rho U^2$ and hence St is calculated by $St = (C_f/2)A$, where $A = Pr^a [1 - (x/x_1)^b]^c$, x_1 is the unheated starting length based on Blasius equation, x is the relative streamwise distance, $C_f/2 = 0.453 Re_x^{-0.5}$, $a = -2/3$, $b = 0.75$ and $c = -1/3$ for laminar analytical solution and $C_f/2 = 0.03 Re_x^{-0.2}$, $a = -0.4$, $b = 0.9$ and $c = -0.11$ for turbulent correlation formula.

As given in Figs. 5 and 6, the Stanton numbers derived from C_f are comparatively smaller than experimental St for all cases, but the difference becomes more apparent at the lower velocity of 4 m/s (Fig. 5), particularly on the convex wall, where the flow is more vulnerable in lower velocities. The gap between experimental and derived St was smallest in the concave and biggest on the convex wall at both flow cases. The fuller velocity profiles resulting in the thinner boundary layers, smaller H and higher $\bar{\gamma}$ on the concave wall corresponded to higher C_f and St than flat plate, particularly at the higher velocity of 12 m/s (Fig. 6). Concave wall data show, particularly for the inlet velocity of 12 m/s, that although the experimental St coincides with the turbulent correlation at the downstream section ($\bar{\gamma} = 0.97$), the C_f-based St value is below the correlation by 12%. Concave wall data of Volino and Simon [13] also indicated a gap of up to 25% among the turbulent analogy and measured C_f at the end of transition. Figure 5 additionally implies that the thickening of boundary layer at 4 m/s with bigger H and lower $\bar{\gamma}$ on the convex wall gave rise to lower C_f and St than those of the flat plate. The difference in the experimental and derived St was associated with convex curvature rather than concave and this became more pronounced at the lower velocity of 4 m/s. The experimental St for the concave wall are close to the records of Wright and Schobeiri [22], moreover, the relative relation of the derived and experimental St is in harmony with the reports of Zhou and Wang [6] and Wang and Simon [18], for the flat and convex surfaces, respectively. Figures 5 and 6 together put forward that different inlet velocities, although either in the transitional region, result in altered St data by 10, 8 and 6% for the convex, flat and concave walls, respectively; similar findings were also

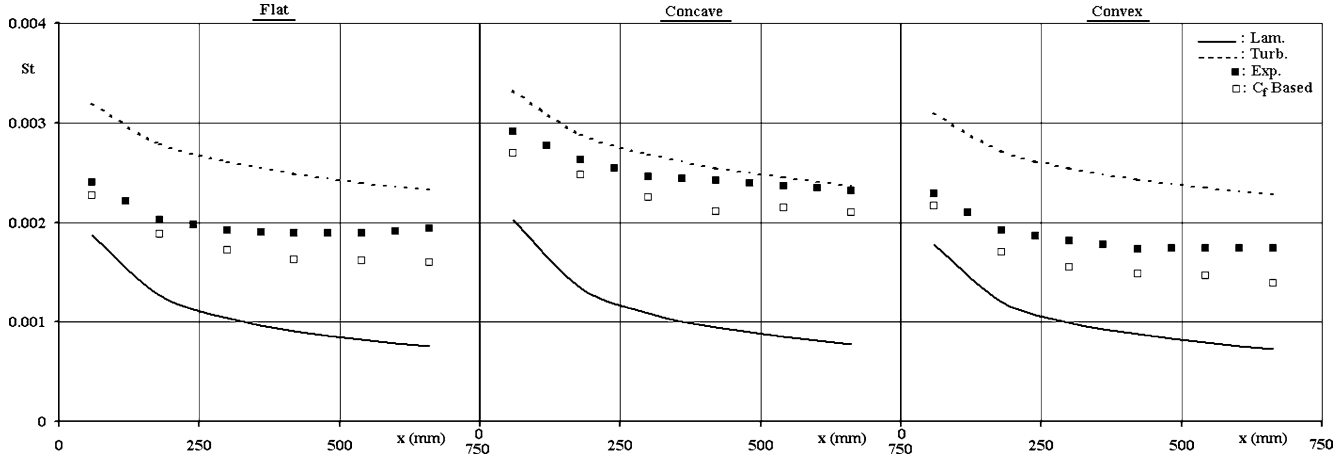

Fig. 6 Streamwise variation of Stanton numbers for $U = 12$ m/s

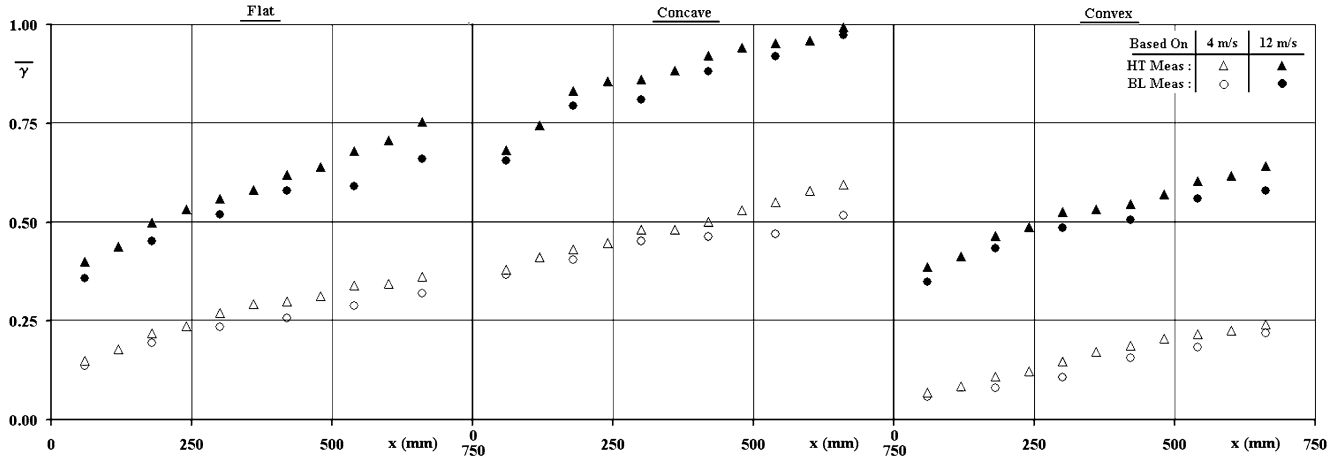

Fig. 7 Streamwise variation of mean intermittency factors

reported by Schook et al. [10] for the flat surface up to 50% and by Turner et al. [23] for the convex wall up to 45%.

Similar to the method of Schook et al. [10], the mean intermittency factor $\bar{\gamma}$ for each location was also found from the experimental St as

$$\bar{\gamma} = \frac{St - St_L}{St_T - St_L} \tag{7}$$

where St_L and St_T are the laminar and turbulent Stanton numbers, evaluated from the analytical solution and turbulent correlation, as shown in Figs. 5 and 6. It is suffice to say that the $\bar{\gamma}$ derived from St was up to 15% higher than those of velocity measurements, particularly at the last measuring station. The bigger $\bar{\gamma}$ values derived from St than that from velocity might be attributed to the influence of hot fluid that moved from wall to core flow, provoking the mechanism of transition. So, the heated wall for the temperature measurements seems likely to be responsible for much of the bigger intermittency and the enhanced transition. It appears that the influence of the heated wall was more effective on the higher velocity than the lower one and led to the expected higher $\bar{\gamma}$, C_f and St. The velocity and temperature measurements showed that the difference between the $\bar{\gamma}$ values derived from velocity and Stanton number of Fig. 7 was also associated with the difference between the derived and the experimental Stanton numbers of Figs. 5 and 6, with a maximum deviation of 8%.

It was concluded that there was no remarkable difference in St at the leading edge among all surfaces, but the difference towards the last measuring station (concave–flat plate and convex–flat plate) become so significant that concave curvature has been linked with increases in St around 22 and 20% and the convex curvature has coincided with a reduction of St up to 12 and 10%, with respect to those of flat plate at 4 and 12 m/s, respectively. These proportions are close to those of Turner et al. [23], who determined a shift of 17% among the flat plate and convex wall St data. The ratio of the concave to convex heat transfer rates is the range of 38–34% and is similar to the establishments of Ligrani and Hedlund [21], who pointed an augmentation of 30%.

4 Conclusion

The laminar to turbulent transition process was experimentally investigated in flat plate, concave and convex wall boundary layers subject to constant heat flux on the flow surface. The experimental observations were compared to those from other relevant investigations so as to discuss the combined effects of surface curvature, inlet velocity and surface heat flux on transition mechanism in conjunction with the boundary layer parameters. It was found that the higher intermittency and the lower shape factor values, recorded on the concave wall, resulted in earlier transition than the flat plate and convex walls. On the other hand, the lower intermittency, the higher momentum thickness Reynolds numbers and the higher shape factor values of the convex wall delayed the transition process so that the convex and the flat surface mean intermittencies remained below 0.25–0.65 and 0.45–0.75 and reached higher values of 0.65–0.97 for the concave wall at 4 and 12 m/s, respectively. The new equation for the estimation of $\bar{\gamma}$ was also developed to calculate the mean intermittency, and compared to the experimental values with an inaccuracy of less than $\pm 2\%$. Heat transfer measurements showed that mean Stanton numbers of the higher velocity remained above those of the smaller one by 10, 8 and 6% for the convex, flat and concave walls, respectively. Moreover, concave curvature caused Stanton numbers to increase up to 22 and 20% and the convex curvature to decrease by 12 and 10%, with respect to those of flat plate at 4 and 12 m/s. Mean intermittency values, derived from Stanton numbers, were found to be higher than those from velocity. As a result, the transition process due to

heated wall took place earlier in all cases and moved the transition onset towards the upstream.

Acknowledgements This work is partly supported by the Uludag University Research Fund.

References

1. Narasimha R (1957) On the distribution of intermittency in the transition region of a boundary layer. J Aerospace Sci 24:711–712
2. Abu-Ghannam BJ, Shaw H (1980) Natural transition of boundary layers—the effects of turbulence, pressure gradient and flow history. Mech Eng Sci 22(5):213–228
3. Cheng KC, Obata T, Gilpin RR (1988) Buoyancy effects on forced convection heat transfer in the transition regime of a horizontal boundary layer heated from below. J Heat Trans—ASME Trans 110:596–603
4. Zumbrunnen DA, Aziz M (1993) Convective heat transfer enhancement due to intermittency in an impinging jet. J Heat Trans—ASME Trans 115:91–98
5. Ciofalo M, Di Piazza I, Stasiek JA (2000) Investigation of flow and heat transfer in corrugated–undulated plate heat exchangers. Heat Mass Trans 36:449–462
6. Zhou D, Wang T (1996) Combined effects of elevated free-stream turbulence and streamwise acceleration on flow and thermal structures in transitional boundary layers. Exp Therm Fluid Sci 12:338–351
7. Wang T, Keller FJ, Zhou D (1996) Flow and thermal structures in a transitional boundary layer. Exp Therm Fluid Sci 12:352–363
8. Johnson MW, Ercan AH (1999) A physical model for bypass transition. Int J Heat Fluid Flow 20:95–104
9. Vasudevan KP, Dey J (2000) Transition zone in constant pressure converging flows. Curr Sci 79(6):821–828
10. Schook R, de Lange HC, van Steenhoven AA (2001) Heat transfer measurements in transitional boundary layers. Int J Heat Fluid Flow 44:1019–1030
11. Zhang DH, Winoto SH, Chew TW (1995) Measurement in laminar and transitional boundary-layer flows on concave surface. Int J Heat Fluid Flow 16:88–98
12. Zhang DH, Chew YT, Winoto SH (1996) Investigation of intermittency measurement methods for transitional boundary layer flows. Exp Therm Fluid Sci 12:433–443
13. Volino RJ, Simon TW (1997) Measurements in a transitional boundary layer with Görtler vortices. J Fluids Eng—ASME Trans 119:562–568
14. Kestoras MD, Simon TW (1998) Conditionally sampled measurements in a heated turbulent boundary layer: curvature and free-stream turbulence effects. Exp Therm Fluid Sci 17:63–70
15. Toe R, Ajakh A, Peerhossaini H (2002) Heat transfer enhancement by Görtler instability. Int J Heat Fluid Flow 23:194–204
16. Volino RJ, Schultz MP, Pratt CM (2003) Conditional sampling in a transitional boundary layer under high freestream turbulence conditions. J Fluids Eng—ASME Trans 125:28–37
17. Muck KC, Hoffman PH, Bradshaw P (1985) The effect of convex surface curvature on turbulent boundary layers. J Fluid Mech 161:347–369
18. Wang T, Simon TW (1987) Heat transfer and fluid mechanics measurements in transitional boundary layers on convex-curved surfaces. J Turbomach—ASME Trans 109:443–451
19. Abu-Qudais M, Haddad OM, Maqableh AM (2001) Hydrodynamic and heat transfer characteristics of laminar flow past a parabolic cylinder with constant heat flux. Heat Mass Trans 37:299–308
20. Webster DR, Degraaff DB, Eaton JK (1996) Turbulence characteristics of a boundary layer over a two-dimensional bump. J Fluid Mech 320:53–69
21. Ligrani PM, Hedlund CR (1998) Transition to turbulent flow in curved and straight channels with heat transfer at high Dean numbers. Int J Heat Mass Trans 41:1739–1748
22. Wright L, Schobeiri MT (1999) The effect of periodic unsteady flow on aerodynamics and heat transfer on a curved surface. J Heat Trans—ASME Trans 121:22–33
23. Turner AB, Hubbe-Walker SE, Bayley FJ (2000) Fluid flow and heat transfer over straight and curved rough surfaces. Int J Heat Mass Trans 43:251–262
24. Ozalp AA, Umur H (2003) An experimental investigation of the combined effects of surface curvature and streamwise pressure gradients both in laminar and turbulent flows. Heat Mass Trans 39:869–876
25. Gostelow JP, Hong G, Walker GJ, Dey J (1994) Modelling of boundary layer transition in turbulent flows by linear combination integral method. ASME Paper No. 94-GT-358
26. Schubauer GB, Klebanoff PS (1955) Contributions on the mechanics of boundary layer transition. NASA TN-3489